EPJ Web of Conferences **287**, 08008 (2023) https://doi.org/10.1051/epjconf/202328708008
EOSAM 2023

Multipass cell post-compression at 515 nm as an efficient driver for a table-top 13.5 nm source

Maximilian Karst [1,2,3,*], *Pauline* Pfaller[1], *Robert* Klas[1,2,3,4], *Mahmoud* Abdelaal[1], *Ziyao* Wang[1], *Jan* Rothhardt[1,2,3,4] and *Jens* Limpert[1,2,3,4]

[1]Institute of Applied Physics, Abbe Center of Photonics, Friedrich Schiller University Jena, Albert-Einstein-Str. 6, 07745 Jena, Germany
[2]Helmholtz-Institute Jena, Fröbelstieg 3, 07743 Jena, Germany
[3]GSI Helmholtzzentrum für Schwerionenforschung, Planckstraße 1, 64291 Darmstadt, Germany
[4]Fraunhofer Institute for Applied Optics and Precision Engineering, Albert-Einstein-Str. 7, 07745 Jena, Germany

Abstract. We present a table-top, efficient and power scalable scheme enabling the effective generation of extreme ultraviolet radiation up to 100 eV photon energy. Therefor ultrashort pulses (< 20fs) in the visible spectral range (515 nm) are used to drive high harmonic generation (HHG) in helium. This allows for a significant efficiency boost compared to near-infrared (NIR) drivers, enabled by the favourable scaling of the single-atom response of λ^{-6} [1]. The experimental realization of a mulitpass cell delivering 15.7 fs pulses with a peak power close to 25 GW at 515 nm and an overall efficiency (IR to compressed green pulse) of >40 %. In conjunction, preliminary HHG results will be presented, paving the way for mW-class HHG sources at 13.5 nm.

1 High flux high harmonic sources

High harmonic generation (HHG) allows for the creation of coherent radiation in the extreme ultraviolet (XUV/EUV) spectral region. The access to this spectral region, through the means of a lab-scale setup, enabled a plethora of applications such as the investigation of electron dynamics in matter [2], spectroscopic analysis [3] and coherent diffractive imaging (CDI) [4]. Where in recent years the spectral region at 92 eV has gained particular interest due to its use in EUV-lithography [5]. Explicitly, actinic metrology of the used masks remains an open question. Here, 13.5 nm ptychography (a form of scanning CDI) poses as an attractive solution. All of the aforementioned applications would benefit from a high photon flux, e.g. to decrease measurement times or increase signal to noise ratios. This can be achieved by an increase in driving laser power, which linearly improves the XUV flux but quickly reaches practicability and cost constraints. However, by simultaneously increasing the HHG efficiency the generated photon flux can be increased dramatically. This can be achieved by using short-wavelength drivers, allowing for a boost in the single-atom response by λ^{-6} [1], e.g. frequency doubling of the driving laser in principle yields a factor of 64. Furthermore, shorter driving pulse durations enable phase matching at higher intensities, resulting in an increased cut off and efficiency [9]. Combining these scaling laws, we believe a high-power ultrafast source in the visible spectral range (VIS) is the optimal driver for high harmonic generation with cut off energies up to 100 eV.

2 Multipass cell post-compression and XUV generation

The scheme we are presenting consists of four building blocks; (1) the driving laser, (2) a nonlinear frequency conversion stage, (3) a consecutive post-compression stage and, finally, (4) the generation of high harmonic radiation. A first experimental realization of this setup is published in [10], which will briefly be covered in the following.

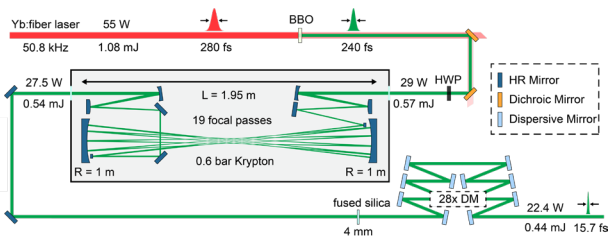

Fig. 1. Schematic of the experimental setup

The driving laser is an Ytterbium fiber laser system delivering 55 W of average power at 50 kHz, corresponding to a pulse energy of 1.1 mJ. The spectrum is centered around 1030 nm with a close to transform-limited pulse duration of 280 fs. Frequency-doubling takes place in a 1.5 mm long BBO-crystal cut for type-I phase matching, yielding 29 W at 515 nm, corresponding to a conversion efficiency of more than 52%. The 240 fs long pulses are guided into a gas-filled Herriot-type multipass cell, where they undergo spectral broadening through self-phase modulation. In 19 focal passes 0.6 bar Krypton provide a sufficient amount of nonlinearity to

* Corresponding author: maximilian.karst@uni-jena.de

fully cover the supported bandwidth of the employed dielectric mirrors. The cavity mirrors are 50 mm in diameter separated by 1.95 m in a concentric geometry. The transmission through the cell is close to 95 %, which is in line with the expected linear losses of the used optics. Temporal recompression is realized through 28 dispersive mirror reflections, with each one providing -100 fs² of group delay dispersion (GDD). The shortest pulse duration is achieved by fine tuning the dispersion with additional 4 mm of fused silica, resulting in a total GDD of approximately -2525 fs². After compression 22.4 W of average power and 0.44 mJ pulse energy are available. Temporal characterization of a sample, split off via two fused silica wedges, is carried out through a commercially available TIPTOE device [11]. The retrieved pulse and spectrum can be seen in Fig. 2., in combination with a grating-based spectrometer measurement and the respective calculated Fourier-limited pulse duration.

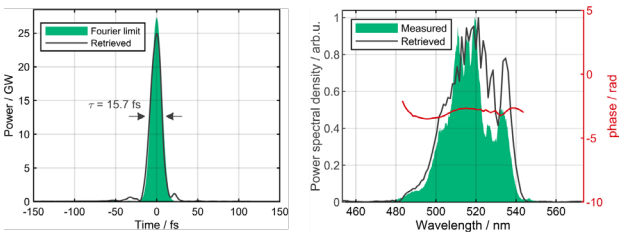

Fig. 2. Temporal characterization of the compressed output pulses via the TIPTOE technique. (Left) Retrieved temporal pulse profile and Fourier limit calculated from the measured spectrum normalized to the output pulse energy. (Right) Measured and retrieved spectrum and corresponding spectral phase.

The retrieved pulse duration of 15.7 fs is within 5 % of the transform-limited pulse duration of 14.9 fs. The retrieved pulse shows a high temporal contrast with more than 93 % of energy in the main feature resulting in a peak power of 24.9 GW. Additionally, an M²-measurement of the compressed and sampled beam reveals a high beam quality with an M²<1.2 in both axis. Overall, the nonlinear frequency conversion and the post-compression stage operate at a total efficiency of more than 40 %.

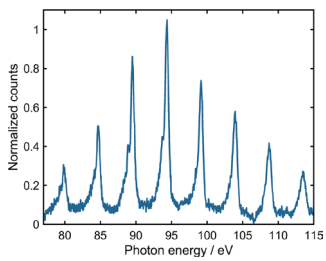

Fig. 3. Normalized HHG spectrum, centred around the 39th harmonic line (94eV).

In the following these pulses are used to generate high harmonic radiation in a helium gas jet, targeting the spectral region around 90 eV. In a preliminary study we were able to push the phase-matched cut-off energy beyond 100 eV through the use of helium as interaction medium (see Fig. 3.). The achieved conversion efficiency at the 39th harmonic (94 eV) was determined to be 1e-8, which is comparable to state-of-the-art systems around 90 eV driven by NIR few-cycle lasers [12].

3 Summary and Outlook

In summary, we report a nonlinear frequency conversion stage followed by a multipass cell based post-compression delivering close to 25 GW of peak power at an overall efficiency of more than 40 %. The combination of ultrashort pulses (< 10 optical cycles) and high peak power enable the phase-matched generation of EUV radiation.

We believe the presented approach will allow for unprecedented amounts of XUV photon flux up to 100 eV photon energy. The inherent advantage of this scheme is the maturity and power scalability of every building block utilized within this demonstration. Ultrafast Yb-fiber lasers have been demonstrated with up to 10 kW of average power [13]. Second harmonic generation to the green spectral range with ultrafast lasers was demonstrated up to 1.4 kW [14], albeit being with picosecond pulses. Multipass cells equally show power scalability to kilowatt level average power [15]. Based on this, power scalability to 100 W and beyond is possible and is currently being investigated. Furthermore, an improvement of the generation conditions (e.g. optimized gas target and focusing geometry) should allow for a boost in conversion efficiency by up to two orders of magnitude. In combination, the improvement in driving source average power and the boost in HHG efficiency should enable photon flux of more than 100 µW per harmonic line at around 90 eV – an increase in EUV average power by two orders of magnitude compared to the state-of-the-art [12, 16].

References

1. A. D. Shiner et al., Phy. Rev. Lett. **103**, 073902 (2009)
2. F. Krausz et al., Rev. Mod. Phys. **81**, 163 (2009)
3. A. C. LaForge et al., J. Phys. B: At., Mol. Opt. Phys. **53**, 244012 (2020)
4. M. Zürch et al., Sci. Rep. **4**, 7356 (2014).
5. C. Wagner et al., Nat. Phot. **4**, 24 (2010)
6. W. Eschen et al., Light: Sci. Appl. **11**, 117 (2022)
7. S. Hädrich et al., J. Phys. B: At., Mol. Opt. Phys. **49**, 172002 (2016)
8. A. G. Ciriolo et al., APL Phot. **7**, 110801 (2022)
9. T. Popmintchev et al., Nat. Phot. **4**, 822–832 (2010).
10. M. Karst et al., Opt. Lett.**48**, 1300 (2023)
11. S. B. Park et al., Optica **5**, 402 (2018)
12. R. Klas et al., Opt. Exp. **28**, 6188 (2020).
13. M. Müller et al., Opt. Lett. **45**, 3083 (2020)
14. C. Röcker et al., Opt. Lett. **45**, 5522 (2020)
15. C. Grebing et al., Opt. Lett. **45**, 6250 (2020)
16. T. Popmintchev et al., Sci. **350**, 1225–1231 (2015)